Adsorption 11: 709–714, 2005
© 2005 Springer Science + Business Media, Inc. *Manufactured in The Netherlands.*

Selenium and Carbon Nanostructures in the Pores of $AlPO_4$-5

THOMAS ROUSSEL, CHRISTOPHE BICHARA AND ROLAND J.-M. PELLENQ*
Centre de Recherches sur la Matière Condensée et Nanosciences, CNRS Case 913, Campus de Luminy,
13288, Marseille Cedex 9, France
pellenq@crmc2.univ-mrs.fr

Abstract. A Tight Binding Grand Canonical Monte Carlo (TB-GCMC) simulation of the adsorption of selenium and carbon in $ALPO_4$-5 zeolite is presented. We show that the structure of confined Se varies from a stretched chain to a piling of Se_5 rings, with intermediate structures combining chains and rings, while that for carbon reveals the mechanism for producing ultra small nanotubes. In the case of selenium, the ring structures are favored at low temperature and high pressures while chains are stable at higher temperatures and lower pressures. The diversity of carbon bonding allows to form chains, in-chain loops that transform into aromatic clusters and eventually tubes. These results are in qualitative agreement with recent experimental results.

Keywords: adsorption, Grand Canonical Monte-Carlo simulation, selenium nanostructures, carbon nanotubes

1. Introduction

Classically, zeolites are used in heterogeneous catalysis and gas separation. They are now involved in the process of manufacturing metallic or semi-conductor nanostructures (clusters, nanowires and nanotubes). After matrix removal (using acid leaching for instance), it is hoped that these nanostructured phases will have interesting (electronic, optical, ...) properties. From a more fundamental point of view, they are good candidates to study low dimension physics. Experimental results for selenium adsorption in zeolites can be found in a series of papers: (Poborchi et al., 1999; Sun et al., 1997; Goldbach et al., 1997; Armand et al., 1997). For carbon, there is an increasing amount of results since the seminal work of Tang et al. (Tang et al., 1997, 2000). Among all available zeolitic structures, those with a neutral framework are of particular interest in modeling since the adsorbed species interact only weakly with the matrix and the electronic structure of the guest can reasonably be assumed to be unaffected by the neighboring host atoms. One leading example of such a structure is silicalite in which Se simulations of adsorption were recently performed (Bichara et al., 2002). Another example of neutral zeolitic structure is $AlPO_4$-5, a zeolite that exhibits a network of parallel channels of about 7.3 Å in diameter. In this work, we present the results of a series of Grand Canonical Monte Carlo simulations of Se and C adsorption in $AlPO_4$-5.

2. Computational Methods

2.1. The Adsorbate-Zeolite Potential Energy

The interaction of selenium or carbon with Al, P and O atoms participating to the zeolite framework is assumed to remain weak, in the physisorption energy range. In this work, we have used a TrAZ form of the original PN-type potential function as originally reported for adsorption of rare gases and nitrogen in silicalite-1 (Pellenq et al., 1994). The PN-TrAZ potential function is based on the usual partition of the adsorption intermolecular energy restricted to two body terms only: it includes a dispersion interaction term, a repulsive short range contribution and an induction term. In the TrAZ model, the adsorbate-surface energy (u_i) of a selenium (or carbon respectively)

---

*To whom correspondence should be addressed.

atom at position i in the simulation box, is given by

$$u_i = \sum_{j\in\{\mathrm{O,Si,H}\}} \left[A_{ij} e^{-b_{ij} r_{ij}} - \sum_{n=3}^{5} f_{2n} \frac{C_{2n,ij}}{r_{ij}^{2n}} \right] - \frac{1}{2}\alpha E_i^2 \tag{1}$$

The sums runs over all atomic sites in the matrix that are oxygen, phosphorus and aluminium atoms. The first term in the sum is a Born-Mayer term representing a two-body form of the short range repulsive energy due to finite compressibility of electron clouds when approaching the adsorbate at very short distance of the pore surface. There is one such a term per pair of interacting species. The repulsive parameters (A_{ij} and b_{ij}) are obtained from mixing rules of like-atoms pairs (see below). The second term in the above equation is a multipolar expansion series of the dispersion interaction in the spirit of the quantum mechanical perturbation theory applied to intermolecular forces. It has been shown that two (and three body) dispersion C_{2n} coefficients for isolated or in-condensed phase species can be obtained from the knowledge of the dipole polarizability and the effective number of polarizable electrons N_{eff} of all interacting species (Pellenq et al., 1998) which are closely related to partial charges that can be obtained from *ab initio* calculations. The f_{2n} terms in the above equation are damping functions of the form:

$$f_{2n} = 1 - \sum_{k=0}^{2n} \left[\frac{(b^{ij} r_{ij})^k}{k!} \right] \cdot e^{-b_{ij} r_{ij}} \tag{2}$$

The role of these damping functions is to avoid divergence of the dispersion interaction at short distance where the wave functions of the two species overlap (i.e. when the interacting species are at contact). The last term in Eq. (1) is the induction interaction as written in the context of the quantum mechanical perturbation theory applied to intermolecular forces (Stone, 1998). It represents an attractive energy arising from the coupling of the polarizable electronic cloud of the adsorbate of polarizability α at position i with the electric field E_i induced by the charges carried by framework species (O, Al and P) that result from the bonding process within the matrix itself. In total, for each adsorbate (Se or C), one has to parametrize three different adsorbate/adsorbent-species potentials; all parameters are given in Table 1. Repulsive parameters for like-pairs are taken from a previous work on the simulation of methane in $\mathrm{AlPO_4}$-5 (Lachet et al., 1996); since atomic selenium has a van der Waals radius very close to that of krypton (2.0 Å; http://www.periodensystem.info/elemente/selen.htm and krypton.htm), we assumed that two selenium atoms will have the repulsive parameters of the Kr-Kr pair ($A_{\mathrm{Kr\text{-}Kr}} = 236.3\ \mathrm{E}_h$ and $b_{\mathrm{Kr\text{-}Kr}} = 1.689\mathrm{a}_0$ (Pellenq et al., 1994). The repulsive interaction parameters for the C-C pair are taken from a previous on adsorption of xylene in faujasite zeolite (Pellenq et al., 1996) and combined to those of the zeolite species.

2.2. The Adsorbate-Adsorbate Interaction Through a Total Energy Model

The adsorbate-adsorbate interaction is described in a tight binding approximation (TB) that is a parameterized version of the Hückel theory. We use a minimal

Table 1. Se-$\mathrm{AlPO_4}$-5 and C-$\mathrm{AlPO_4}$-5 potential parameters.1 $E_h = 27.211$ eV and 1 $\mathrm{a}_0 = 0.529177$ Å.

	Se-O	Se-Al	Se-P	C-O	C-Al	C-P
$C_6(E_h a_0^6)$	89.330	22.910	41.55	36.580	9.3780	17.032
$C_8(E_h a_0^8)$	2536.0	520.80	1132.4	834.82	162.44	371.76
$C_{10}(E_h a_0^{10})$	65430	–	–	20100	–	–
$A(E_h)$	603.80	1264.7	714.30	234.68	491.89	277.57
$b(a_0)$	1.9070	2.7742	3.0410	1.9440	2.8650	3.1340

Se properties		C properties	
Polarizabilities Se (ao^3) 24.5	Number of polarizable electrons $N_{\mathrm{eff}} = 5.63$	Polarizabilities C (ao^3) 9.80	Number of polarizable electrons: $\mathrm{N_{eff}} = 2.65$

Zeolite partial charges		
$q(\mathrm{O}) = -0.78\bar{e}$	$q(\mathrm{Al}) = +1.39\bar{e}$	$q(\mathrm{P}) = +1.77\bar{e}$

s, p_x, p_y and p_z atomic orbital basis set and a Slater Koster parameterization to build the Hamiltonian matrix describing the interaction. To avoid the time consuming diagonalization of this matrix, we use the recursion method to calculate the local density of electronic states on each atom. We restrict the continued fraction expansion at the fourth moment's level which means that only first and second neighbors of each site are taken into account to calculate the band energy term. This approximation is quite crude but captures the quantum nature and the directionality of bonding in selenium and in carbon compounds (from sp to sp^3 hybridization). As usual in the TB formalism (or in the Hückel theory for chemical bonding), a repulsive term prevents the unphysical collapse of matter. The model for Se-Se and C-C interactions then takes the general form:

$$E_{\text{tot}} = E_{\text{band}} + E_{\text{rep}} + E_{\text{disp}} \tag{3}$$

$$E_{\text{tot}} = \sum_i \int_{-\infty}^{E_f} E n_i(E) dE + \sum_{j>i} V_0 \left(\frac{1}{r_{ij}}\right)^p F_1(r_{ij}) - F_2(r_{ij}) \frac{C_6}{r_{ij}^6} \tag{4}$$

where r_{ij} is the interatomic distance between sites i and j, $n_i(E)$ is the local density of state on site i, E_f is the Fermi level and C_6 is the constant of the dispersion term restricted to the dipole-dipole interaction (see equation (1)) and calculated from the polarizability of Se and a number of polarizable electrons (see Table 1). $F_1(r_{ij})$ and $F_2(r_{ij})$ are damping functions (see Eq. (2)). For selenium, the values of V_o, p and the parameters defining the resonance integrals (not shown here) are given in Bichara et al. (1998). This model was shown to accurately describe Se thermodynamic properties (liquid–vapor equilibrium line, critical point) of bulk selenium. For carbon, it will be presented in a separate publication (Amara et al., 2004) and does not include a dispersion term.

2.3. *Simulation Technique*

We performed standard Grand Canonical Monte Carlo (GCMC) simulations (Pellenq et al., 1995) on a periodic box containing 11 orthorhombic unit cells of AlPO$_4$-5 for selenium stacked along the pore axis in order to calculate adsorption isotherms and determine the adsorption mechanism. Starting with a Se$_2$ or C$_2$ dimer located in the central channel, we gradually raised the chemical potential and recorded the average number of adsorbed atoms. The chemical potential of Se and C is referred to a fictitious monoatomic ideal gas. This explains the large values of the chemical potential at which the adsorption takes place (see below): between -3.0 and -2.2 eV/atom for Se and between -5.5 and -6 eV/atom for C respectively. As expected in the temperature range of the simulations, these values are only slightly larger than the bond energy of Se (-2.25 eV/atom) and C (-7 eV); the contribution of the configurational entropy to the chemical potential being small. A minimum of $5 \cdot 10^5$ Monte Carlo macro-steps was performed, each macro-step consisting of randomly performing 1000 attempted displacements, 10 attempted insertion and 10 attempted removals of an adsorbate atom. In order to accelerate GCMC simulation runs, we calculated the adsorbate/substrate interaction using an energy grid, which splits the simulation box volume into a collection of voxells. The adsorbate/substrate potential energy was calculated at each corner of each elementary cube (about 0.2^3 Å^3). The adsorbate/substrate energy is then obtained by an interpolation procedure of the 3D energy grid. This procedure allows simulating adsorption with no direct summation over the matrix species in GCMC runs and is computationally very efficient (Pellenq et al., 1995).

3. Results and Discussion

3.1. *Selenium Adsorption*

We show in Fig. 1 the adsorption isotherms of Se in AlPO$_4$-5 at three different temperatures. The stability of chain structures at high temperature and relatively low chemical potential is a consequence of the larger vibrational entropy of the chains and the gradual transition to a ring structure results from the larger number of Se atoms that can be packed when the chemical potential is increased. We may assume that a ring to chain transition with increasing temperature (polymerization of Se rings) should proceed with increasing temperature, but we have not yet observed it directly upon heating a ring structure or cooling a chain structure. The adsorption branches calculated at 190°C and 420°C are very similar: the channels are either empty or full and the transition is sharp. The adsorbed Se phase is a piling of Se$_5$ (sometimes Se$_6$) rings perpendicular to the axis of the channel. When the channel is completely filled, it corresponds to 2 Se$_5$ rings per channel per unit cell, yielding a total number of 20 Se atoms per unit cell of AlPO$_4$-5. The

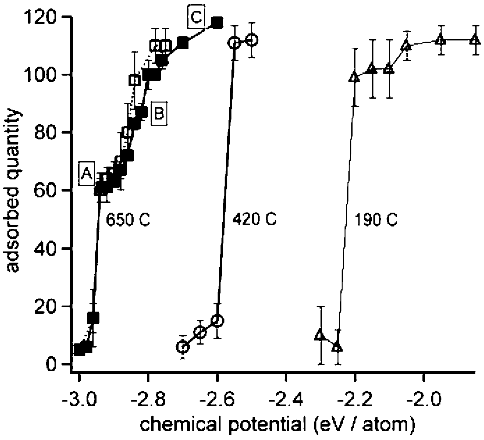

Figure 1. Se Adsorption isotherms calculated at $T = 190°\mathrm{C}$ (triangles), 420°C (circles) and 650°C (full squares); open squares: desorption. Points A and C correspond to the configurations discussed in the text and displayed on Fig. 2(a) and (b).

three points at low fillings on the isotherm at 420°C correspond to 1, 2 and 3 rings respectively. They are probably metastable since there is no obvious reason why such a situation should be stable. It is therefore possible that the step on the adsorption isotherm should lie at a lower chemical potential value. The situation is quite different at 650°C: a sharp transition takes place between the nearly empty channel and a half filled channel (point A in Fig. 1), followed by a gradual, almost reversible, increase of the adsorbed quantity with increasing chemical potential. The structure of the adsorbed phase is a mixture of chains and rings. Analysis of equilibrium configurations reveals that a stretched chain 'fills' the channel on point A (see Fig. 2(a)), and that this chain becomes more squeezed (like a compressed spring) up to point B and, due to this compression of the chains, more and more rings (that maximize the filling of the channels) are formed up to point C (see Fig. 2(b)). The results of the simulations indicate that the incorporation of Selenium into the channels of AlPO4-5 zeolite is indeed more complex than a simple filling of the channels by chains similar to the chains forming the structure of crystalline bulk selenium. At low temperature a ring structure is clearly favored, not only because it allows a larger number of Se atoms to be adsorbed, but also during the growth of the adsorbed phase. At low temperatures, even at partial fillings, Se prefers rings structures. This is the reason why the convergence of the calculations is so long to obtain. Once a series of rings is formed, the nucleation of another ring close to an existing one is a rare event that proceeds by forming a 3-fold connection from which a piece of chain grows. This chain then splits from the originating ring to form one or several rings that are more stable. We observe a majority of Se$_5$ and occasionally Se$_6$rings but no larger ring species. The structure of confined Se thus varies from a stretched chain to a piling of Se$_5$ rings, with intermediate structures combining chains and rings; the ring structures being favored at low temperature and high pressures while chains are stable at higher temperatures and lower pressures. The stability of chain structures at high temperature and relatively low chemical potential is a consequence of the larger vibrational entropy of the chains and the gradual

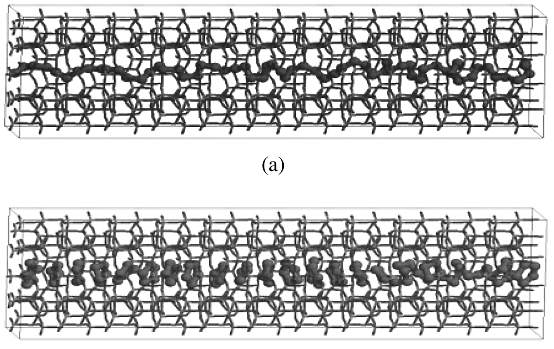

(a)

(b)

Figure 2. (a) Snapshot of a typical configurations obtained at $T = 650°\mathrm{C}$ (points A on Fig. 1), 62 Se, $\mu =-2.94$ eV/atom. (b) Snapshot of a typical configurations obtained at $T = 650°\mathrm{C}$ (points C on Fig. 1), 111 Se, $\mu = -2.70$ eV/atom.

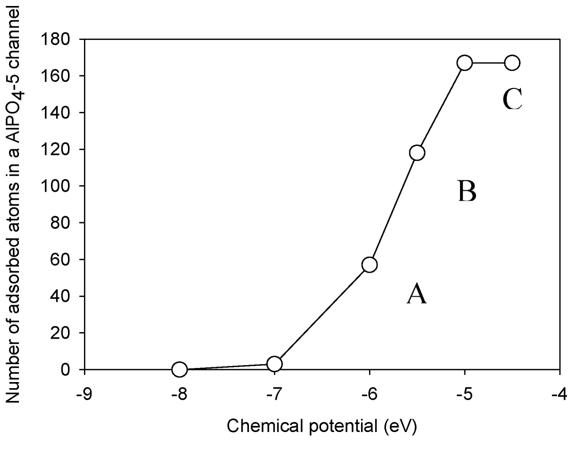

Figure 3. C adsorption isotherms calculated at $T = 727°\mathrm{C}$. Points A ($\mu = -6$), B ($\mu = -5.5$) and C ($\mu = -5$) correspond to the configurations discussed in the text and displayed on Fig. 4(a), (b) and (c).

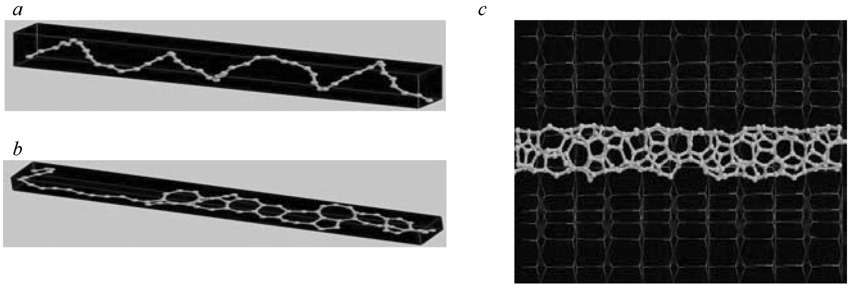

Figure 4. Equilibrium configurations for carbon adsorption at points A, B, C along the adsorption isotherm at 1000 K.

transition to a ring structure results from the larger number of Se atoms that can be packed when the chemical potential is increased. We may assume that a ring to chain transition with increasing temperature (polymerization of Se rings) should proceed with increasing temperature, but we did not observe it directly upon heating a ring structure or cooling a chain structure.

3.2. *Carbon Adsorption*

An adsorption isotherm of carbon at 1000 K in $AlPO_4$-5 is shown in Fig. 3 as a preliminary study of carbon adsorption in inorganic matrices. The carbon growth begins with a helicoidal chain composed of 48 atoms that gradually includes loops and transforms in a Single Wall Nano-Tube (SNWT) with a diameter of ∼4Å composed of five, sixth and seven atom rings in agreement with recent experimental results (Tang et al., 2001). Carbon bonding differs from that of selenium because of the value of the bond energy and its ability to form different (sp, sp^2 , sp^3) bonds. This is illustrated in Fig. 4(a)–(c). The structures were thermalized at 2000 K in order to cure defects. The bond angle and neighbors distributions show a decrease of defects in the nanotubes. We have tested the effects on the chemical potential increment and shown that low pressure and temperature conditions are needed to obtain the more stable structures during the CVD adsorption process.

Conclusion

We have performed GCMC simulations of Chemical Vapour Deposition of Se and C in zeolite $AlPO_4$-5 based on a tight binding model for the adsorbate-adsorbate interactions able to account for adsorbate-adsorbate convalent bonding along with a realistic model for adsorbate-substrate interactions. This gives a direct access to adsorption thermodynamics and mechanism. The GCMC results show that the structure of Se incorporated into $AlPO_4$-5 zeolite is not simple but ranges from a etched chain structure to a piling of Se_5 rings, with mixed intermediate structures. They suggest that a polymerization transition might occur upon temperature. In the case of C adsorption, a possible growth mechanism proceeds through a three step mechanim: chain, close-loop-containing chains and eventually an ultra small nanotube of 0.4 nm in diameter, in agreement with experiment.

References

Amara, H., J.-M. Roussel, F. Ducastelle, and C. Bichara, to be published.

Armand, P., M.-L. Saboungi, D.L. Price, L. Iton, C. Cramer, and M. Grimsditch, "Nanoclusters in Zeolite," *Phys. Rev. Lett.*, **79**, 2061–2064, (1997).

Bichara, C., J.-M. Raty, and J.-P. Gaspard, "Structure of High Temperature Fluid Selenium," *J. Non Cryst. Sol*, **250**, 419–422 (1999).

Bichara, C., R.J.-M. Pellenq, and J.-Y. Raty, "Adsorption of Selenium Wires in Silicalite-1 Zeolite: A First Order Transition in Microporous Solids," *Phys. Rev. Lett.*, **89**, 16102–16106 (2002).

Goldbach, A., L.E. Iton, and M.-L. Saboungi, "Formation of Isolated Se_8 Rings in Zeolites," *Chem. Phys. Lett.*, **281**, 69–73 (1997).

Lachet, V., A. Boutin, R.J.-M. Pellenq, D. Nicholson, and A.H. Fuchs, "Molecular Simulation Study of the Structural Rearrangement of Methane Adsorbed in Aluminophosphate $AlPO_4$-5," *J. Phys. Chem.*, **100**, 9006–9013 (1996).

Li, I.L., P. Launois, and Z.K. Tang, "Synthesis and Characterization of Se Nanostructures Inside Porous Zeolite Crystals," *J. Applied Surf. Sci.*, **226**, 36–40 (2004).

Pellenq, R.J.-M. and D. Nicholson, "Potential Function for Rare Gases Interacting with Silicalite-1 Zeolite," *J. Phys. Chem.*, **98**, 13339–13349 (1994).

Pellenq, R.J.-M. and D. Nicholson, "Grand Ensemble Monte-Carlo simulation of Simple Molecules Adsorbed in Silicalite-1 Zeolite" *Langmuir*, **11**, 1626–1635 (1995).

Pellenq, R.J.-M., B. Tavitian, D. Espinat, and A.H. Fuchs, "Grand Canonical Monte-Carlo Simulations of Adsorption of Polar and Non Polar Molecules in NaY Zeolite," *Langmuir*, **12**, 4768–4783 (1996).

Pellenq, R.J.-M. and D. Nicholson, "A Simple Method for Calculating Dispersion Coefficients for Isolated and Condensed-Phase Species," *Mol. Phys.*, **95**, 549–570 (1998).

Poborchii, V.V., A.V. Kolobov, J. Caro, V.V. Zhuravlev, and K. Tanaka, "Dynamics of Single Selenium Chains Confined in One-Dimensional Nanochannels of $AlPO_4$-5: Temperature Dependencies of the First and Second-Order Raman Spectra," *Phys. Rev. Lett.*, **82**, 1955–1958, (1999).

Stone, A., "The Theory of Intermolecular Forces," International Series of Monographs on Chemistry, Clarendon Press, 1997.

Sun, H.D., Z.K. Tang, W.M. Zhao, and G.K.L. Wong, "Temperature Dependence of Excitonic Energy in Isolated Se Chains formed in Channels of $AlPO_4$-5 Crystals," *Appl. Phys. Lett.*, **71**, 2457–2459 (1997).

Wang, N., Z.K. Tang, G.D. Li, and J.S. Li, "Single-Walled 4 Å Nanotube Arrays," *Nature*, **408**, 50–51(2000).